

# Climate and geology overwrite land use effects on soil organic nitrogen cycling on a continental scale.

Lisa Noll<sup>1,2</sup>, Shasha Zhang<sup>1</sup>, Qing Zheng<sup>1</sup>, Yuntao Hu<sup>1,3</sup>, Florian Hofhansl<sup>4</sup> and Wolfgang Wanek<sup>1\*</sup>

<sup>1</sup>Division of Terrestrial Ecosystem Research, Department of Microbiology and Ecosystem Science, Center of Microbiology and Environmental Systems Science, University of Vienna, Vienna, Austria

<sup>2</sup>German Environment Agency, Dessau-Rosslau, Germany

<sup>3</sup>Lawrence Berkeley National Laboratory, Berkeley, USA

<sup>4</sup>International Institute for Applied Systems Analysis, Schlossplatz 1, A-2361 Laxenburg, Austria

*Correspondence to:* Wolfgang Wanek (wolfgang.wanek@univie.ac.at)

**Abstract.** Soil fertility and plant productivity are globally constrained by N availability. Proteins are the largest N reservoir in soils and the cleavage of proteins into small peptides and amino acids has been shown to be the rate limiting step in the terrestrial N cycle. However, we are still lacking a profound understanding of the environmental controls of this process. Here we show that integrated effects of climate and soil geochemistry drive protein cleavage across large scales. We measured gross protein depolymerization rates in mineral and organic soils sampled across a 4000-km-long European transect covering a wide range of climates, geologies and land uses. Based on structural equation models we identified that soil organic N cycling was strongly controlled by substrate availability, e.g. by soil protein content. Soil geochemistry was a secondary predictor, by controlling protein stabilization mechanisms and protein availability. Precipitation was identified as the main climatic control on protein depolymerization, by affecting soil weathering and soil organic matter accumulation. In contrast, land use was a poor predictor of protein depolymerization. Our results highlight the need to consider geology and precipitation effects on soil geochemistry when estimating and predicting soil N cycling at large scales.

## 1 Introduction

Microbial decomposition of soil organic matter is a fundamental driver of soil ecosystem functions and services, e.g. nutrient regeneration through decomposition maintains soil fertility and plant productivity. For example, the extracellular cleavage of plant- and microbial-derived soil proteins, chitin or peptidoglycan to small organic compounds such as peptides, amino acids and amino sugars regulates organic N uptake by soil microbes, contributes to plant N nutrition and further drives terrestrial inorganic N cycling (Hu et al., 2018; Noll et al., 2019b). Proteins account for up to 90 % of soil N (Martens and Loeffelmann, 2003; Schulten and Schnitzer, 1997). Protein depolymerization is mediated by extracellular enzymes and facilitates microbes and plants to utilize the by far single largest N reservoir in soils. However, the large-scale controls of gross protein depolymerization are largely unknown. Since protein depolymerization is mediated by extracellular enzymes this process is expected to be either enzyme-limited or substrate-limited and thereby to be tied to soil geochemistry and vegetation affecting substrate availability, and to microbial community composition and microbial N demand driving enzyme production (Sinsabaugh et al., 2008).

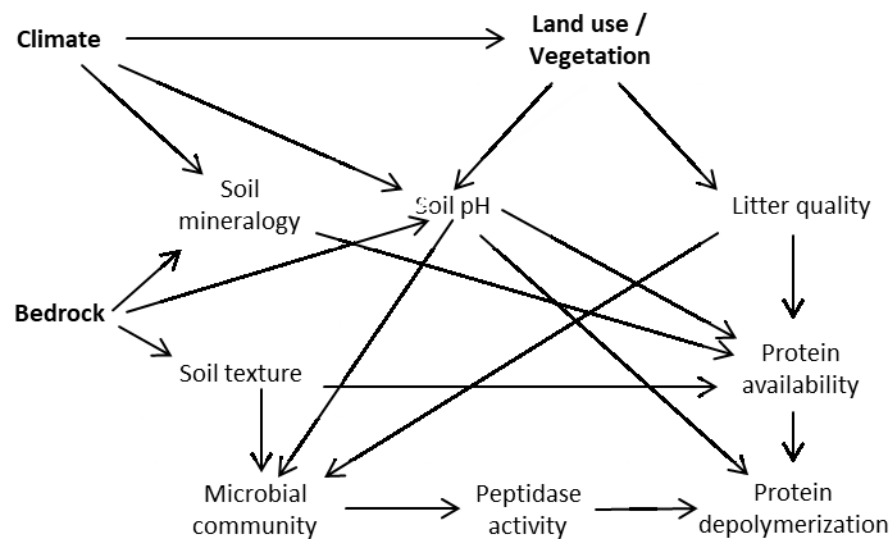
36 Microbial community structure may influence protein depolymerization through several pathways. Across  
37 biogeographic regions peptidase activity increases strongly with soil pH, since the pH optima of most proteolytic  
38 enzymes is about 7 – 8 (Sinsabaugh et al., 2008; Hendriksen et al., 2016). However, soil pH is a major control on  
39 bacterial community composition, and cross-continental studies showed that this pattern is consistent across soil  
40 types and biomes (Lauber et al., 2009; Rousk et al., 2010; Fierer and Jackson, 2006). Given the large difference in  
41 the excreted enzyme complement between microbial taxa, soil nutrient status and edaphic properties (e.g. soil pH,  
42 texture and cation exchange capacity) were shown to shape the set of excreted proteolytic enzymes (Lauber et al.,  
43 2009; Lauber et al., 2008; Jangid et al., 2008; Fuka et al., 2008) by their effects on microbial community  
44 composition. Effects of climate on peptidase activity are mainly indirect, indicated by shifts in vegetation type and in  
45 soil nutrient stoichiometry from low to high latitudes (Hendriksen et al., 2016; Sinsabaugh et al., 2008; Peng and  
46 Wang, 2016). Soil C:N ratios are typically higher in forest soils than in agricultural soils, and affect in particular the  
47 fungi: bacteria ratios (Lauber et al., 2008). Land use can consequently affect the production of soil extracellular  
48 enzymes through its effect on microbial community composition, but also reflecting the external inputs of fertilizer  
49 and lime and soil management (e.g. ploughing), which deplete organic N reservoirs in soils and down-regulate  
50 extracellular N-mining enzyme activities (Jangid et al., 2008; Xiao et al., 2018; Chen et al., 2022; Padbhushan et al.,  
51 2022).

52 Substrate availability is likely the most striking control on organic N depolymerization rates and has been  
53 shown to be driven by land use and soil properties at the regional scale (Noll et al., 2019b). Soil N stocks (as proxy  
54 for soil protein contents) are typically increasing with mean annual precipitation and decrease with the level of  
55 aridity (Delgado-Baquerizo et al., 2013; Marty et al., 2017; Callesen et al., 2007). Changes in temperature and  
56 precipitation patterns are associated with changes of the potential natural vegetation, where N becomes progressively  
57 limiting with vegetation changes from deciduous to coniferous shrubs and trees, and from low to high latitudes  
58 (Kang et al., 2010; Reich and Oleksyn, 2004). Moreover, soil N stocks decrease with intensification of land  
59 management, from forests to grasslands and croplands (Six and Jastrow, 2002). Decomposition experiments of plant  
60 litter and organic soils showed an inverse relationship of gross protein depolymerization rates and resource C:N  
61 ratios and a positive relation with resource N content, though none with potential peptidase activities, suggesting that  
62 protein depolymerization is rather controlled by substrate availability than by the pool size of extracellular enzymes  
63 (Mooshammer et al., 2012). However, in mineral soils the former relationship was less pronounced, indicating that  
64 protein stabilization on mineral surfaces may restrict soil protein cleavage (Wild et al., 2013; Noll et al., 2019b).

65 In mineral soils, organic nitrogen availability is constrained by interactions of organic compounds with the  
66 soil matrix, e.g. by the formation of organo-mineral associations, and restricted accessibility in small pores and soil  
67 aggregates render soil organic matter to become protected from enzymatic attack (Kögel-Knabner et al., 2008;  
68 Quiquampoix, 2000). Stabilization mechanisms are controlled by soil texture and soil mineral assemblage, and  
69 particularly by the amounts of Fe- and Al- (oxyhydr)oxides, which are major sorption sites of soil organic matter in  
70 soils (Kaiser and Guggenberger, 2000). Their amount and composition are shaped by soil parent material (primary  
71 minerals) and environmental conditions during pedogenesis, which control bedrock weathering and the formation of  
72 secondary minerals. Both, protein availability and proteolytic activity are further constrained by

73 substrates/exoenzymes being inactivated by formation of metal-organic complexes or by the complexation with  
74 tannins (Nierop et al., 2002; Peter J Hernes, 2001; Adamczyk et al., 2009).

75 Land use, bedrock and biogeographic region are therefore key controls on soil nutrient status and edaphic  
76 properties and affect microbial community structure, substrate availability and microbial N and C demands (Lauber  
77 et al, 2008; Lauber at al., 2009; Xu et al., 2013, Elrys at al., 2021). Changes in environmental conditions might  
78 thereby be translated into altered organic N process rates (Figure 1). To investigate the major controls on organic N  
79 cycling, we sampled a large-scale transect across Europe, from the Mediterranean to the Subarctic, covering three  
80 different land use types (forest/shrubland, grassland and cropland) as well as a wide range of climates and geologies,  
81 and determined gross protein depolymerization rates using an isotope pool dilution approach targeting soil amino  
82 acid production (protein depolymerization).



83

84 **Figure 1 Proposed model relating climate, bedrock and land use effects to protein depolymerization rates.**

85 We hypothesized that (I) protein depolymerization is restricted by lower soil organic matter content and microbial  
86 activity in cropland soils compared to grassland and forest soils. (II) We further expected that the availability of  
87 proteins and thereby gross protein depolymerization rates are controlled by soil geochemical properties (e.g. soil  
88 pH), mineral assemblage and texture. (III) We further hypothesized that climate is a rather indirect control on organic  
89 N cycling by its effects on vegetation and soil geochemistry as well as on soil N stocks.

## 90 **2 Materials and Methods**

### 91 **2.1 Sampling**

92 Soil samples were collected during summer 2017 (May to August) at the peak of the growing season across a  
93 European continental transect from the warm Mediterranean to the cold Subarctic and from the humid Atlantic  
94 western climate to the dry continental steppes in Romania (Figure 2). The sampled soils were distinct in soil parent  
95 material, soil type, land use and vegetation. Sampling sites were selected to represent the natural vegetation as  
96 defined in the ‘Map of the natural vegetation of Europe’ (Bohn and Katenina, 2000). For each sampling site climate

97 data scaled to 100 m were extracted from the WorldClim database vs. 1.4 (Fick and Hijmans, 2017). Bedrock was  
98 obtained from the international geological map of Europe (IGME5000, 1:5.000.000 (Asch, 2005)) and dominant soil  
99 types were obtained from the “Soil regions of European Union and adjacent areas” map (EUSR5000, 1:5.000.000,  
100 (Bgr [Bundesanstalt Für Geowissenschaften Und Rohstoffe], 2005).  
101 For statistical analyses bedrock types were binned into three groups: limestone, sediment and silicate. Sediment  
102 geologies included Flysch, Molasse, till and fluvial sand, silicate bedrock included plutonic, igneous and

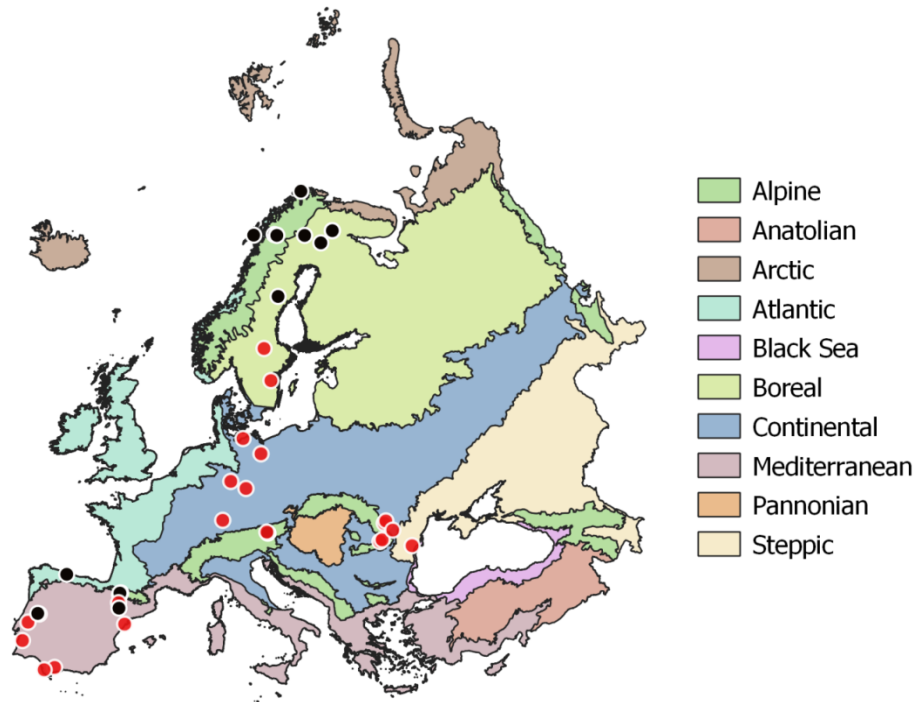


**Figure 2 Sampling sites across European biogeographical regions. Red circles symbolize sampling sites including three land use types (woodland, grassland, cropland). Map of European biogeographical regions was obtained from biogeographical regions dataset of the European Environment Agency.**

103 metamorphic formations, and carbonate bedrock ranged from dolomite to limestone and marl. Mean annual  
104 temperature (MAT) of the sampling sites ranged from -3.5 to 17.8 °C and mean annual precipitation ranged from 415  
105 to 1396 mm y<sup>-1</sup>. Where possible, all three management types (woodland/forest, grassland and cropland) as well as  
106 mineral and organic soils were sampled in close vicinity. In the following we only use ‘woodland’ for subarctic  
107 tundra, open woodlands and forests. At each site bulk samples of mineral top soil (0-15 cm) were taken with a soil  
108 corer (5 cm). Each bulk soil sample consisted of five replicates with about 5 m distance from each other. In total we  
109 sampled 96 mineral top soils from 43 sites. 23 sites included woodland, grassland and cropland soils (Table S1).  
110 Organic layers were sampled at 13 sites using a 20 x 20 cm frame to cut out the organic horizon down to the mineral  
111 soil surface. The depth of the individual organic horizons varied from 2 to 30 cm. Representative leaf litter samples  
112 were collected at each site and represent the dominating vegetation. Roots and stones were removed from the soil  
113 samples manually immediately after sampling. Soil samples, roots, stones and litter samples were cooled (4-8 °C)  
114 and shipped within 3 to 7 days to the University of Vienna for further analyses. Soil samples were homogenized by

115 sieving to 2 mm and separate aliquots were air dried or stored moist at 4 °C. Litter and root samples were washed  
116 and dried in a drying oven at 60 °C.

## 117 **2.2 Basic soil parameters**

118 Soil texture, CaCO<sub>3</sub> content, cation exchange capacity (CEC), base saturation (BS) and exchangeable Ca<sup>2+</sup>, Mg<sup>2+</sup>, K<sup>+</sup>,  
119 Na<sup>+</sup>, Al<sup>3+</sup>, Fe<sup>3+</sup> and H<sup>+</sup> were determined by the Austrian Agency for Health and Food Safety (AGES) according to  
120 European and international standards (ÖNORM). Fe- and Al-oxyhydroxides were determined in acid ammonium  
121 oxalate and in Na-dithionite extracts (Loeppert, 1996) at the Institute of Soil Research (IBF, University of Natural  
122 Resources and Life Sciences, Vienna, Austria). Oxalate extractable Fe (Fe<sub>oxalate</sub>) and Al (Al<sub>oxalate</sub>) refers to amorphous  
123 Fe- and Al oxyhydroxides and Fe bound in organo-metal complexes. Dithionite extractable Fe minus oxalate  
124 extractable Fe represents Fe bound in crystalline oxyhydroxides (Fe<sub>d-o</sub>). The ratio of oxalate extractable Fe over  
125 dithionite extractable Fe presents a measure of the activity of the Fe-mineral phase (Fe<sub>o/d</sub>). To determine the soil  
126 water content, sieved soils were dried at 85 °C for 48 h. Water holding capacity (WHC) was measured by repeatedly  
127 saturating 10 g field-moist soil with deionized water and draining in between for 2.5 hours in a funnel with an ash-  
128 free cellulose filter paper. Field-moist soils were either adjusted to 60% WHC by gentle drying at room temperature  
129 or by addition of deionized water. Before further analyses all soils were pre-incubated for two weeks at 20 °C and  
130 60% water holding capacity (WHC) in PE-Ziploc bags. Soil pH was measured in water and 10 mM CaCl<sub>2</sub> (1 : 5 (w :  
131 v)) using an ISFET pH sensor (Sentron, Leek, The Netherlands). To determine total C and total N in root and litter as  
132 well as soil organic C (SOC) and soil total N (TN) oven dried root, litter and soil samples were ground with a ball  
133 mill (MM 200, Retsch, Germany) and analyzed by an Elemental analyzer (Carlo Erba 1110, CE Instruments)  
134 coupled to a Delta<sup>Plus</sup> Isotope Ratio Mass Spectrometer (Finnigan MAT, Germany) via a ConFlo III interface  
135 (Thermo Fisher, Austria). If necessary, carbonates were removed from soil samples with 2 M HCl prior to SOC and  
136 TN measurements. Soil total P (TP) and soil total inorganic P (TIP) were determined in 0.5 M H<sub>2</sub>SO<sub>4</sub> extracts of  
137 ignited (450 °C, 4 °C (Lajtha et al., 1999)) and control soil aliquots followed by malachite green measurements of  
138 reactive phosphate (Kuo, 1996). Total soil organic P (TOP) was calculated as the difference of TP – TIP. Soils were  
139 extracted with 1 M KCl (1:5 (w:v)) for 1 h and filtered through ash-free cellulose filters (Whatmann). Dissolved  
140 organic C (DOC) and total N (TDN) were measured in the extracts by a TOC/TN analyzer (TOC-VCPh/TNM-1,  
141 Shimadzu, Austria). NH<sub>4</sub><sup>+</sup> and NO<sub>3</sub><sup>-</sup> were measured colorimetrically in the same extracts (Hood-Nowotny et al.,  
142 2010). Dissolved organic N (DON) was calculated as TDN minus NO<sub>3</sub><sup>-</sup> and NH<sub>4</sub><sup>+</sup>. Free amino acids (FAA) were  
143 determined fluorimetrically in 1 M KCl extracts by the OPAME fluorescence method (Jones et al., 2002) as modified  
144 by Prommer et al. (2014). Dissolved inorganic P (DIP, Olsen P) was extracted with 0.5 M NaHCO<sub>3</sub> (1 : 7.5 (w : v),  
145 pH 8.5) for 1 h, filtered through ash free cellulose filters and measured by malachite green. Total dissolved P (TDP)  
146 was measured following acid persulfate digestion and dissolved organic P (DOP) was calculated as the difference of  
147 P concentration between digested and non-digested samples (Lajtha et al., 1999). Soil microbial community  
148 composition was analyzed by phospholipid fatty acid (PLFA) analyses according to Kaiser et al. (2010) and Hu et al.  
149 (2018). Microbial C, N and P were determined by chloroform fumigation extraction (Brookes et al., 1985). Sample  
150 aliquots were fumigated for 48 h and subsequently extracted as described above with 1 M KCl or 0.5 M NaHCO<sub>3</sub>.  
151 Potential activities of leucine-amino peptidase (EC 3.4.11.1) were determined in buffered (Na-acetate, pH 5.5) and

152 unbuffered (ultra-pure water) soil slurries using L-leucine-7-amido-4-methyl coumarin (AMC-leucine) as substrate  
153 (Kaiser et al., 2010). Triplicates of each sample were incubated for 2 h at 25 °C and measured every 30 min.  
154 Fluorescence was measured with a TECAN InfiniteR M200 (Austria) spectrophotometer at an excitation wavelength  
155 of 365 nm and an emission wavelength of 450 nm, and was corrected for sample blank fluorescence and quenching  
156 prior to calculations of AMC concentration.

### 157 **2.3 NaOH extractable protein**

158 2 g of fresh soil were extracted with 0.5 M NaOH (1 : 10 (w : v)) for 2 h in an ultra-sonic bath (160 W, Sonorex  
159 RK510, Germany) and subsequently for further 16 h on a rotary shaker. NaOH extracts free and loosely bound  
160 proteins e.g from organo-mineral associations but not proteins stabilized in metal-organo complexes (Wattel-  
161 Koekkoek et al., 2001). Extracts were centrifuged for 15 min at 1600 x g. As high salt concentrations interfere with  
162 the consequent measurement of hydrolyzed amino acids, 2.5 ml of supernatant were desalted using Sephadex™ G-25  
163 columns (PD10 GE Healthcare, Uppsala, Sweden). For determination of total amino acids we adopted a method  
164 published by Martens and Loeffelmann (2003) and Hu et al. (2018). The purified extracts were freeze-dried and re-  
165 dissolved in 1.5 ml methanesulfonic acid (4 M MSA). 1 ml of samples, bovine serum albumin (BSA) standards, and  
166 blanks were hydrolyzed in an autoclave for 1 h at 135 °C. Hydrolyzed extracts were neutralized with 4 M KOH and  
167 measurements were performed on an HPLC system (Dionex ICS-3000, Thermo Fisher Scientific, Bremen, Germany)  
168 coupled to an electrochemical detector. Amino acids were separated using a PA-10 IC column (Thermo Fisher  
169 Scientific, Bremen, Germany). NaOH-extractable protein (Protein<sub>NaOH</sub>) was calculated as the sum of the 20 measured  
170 amino acids.

### 171 **2.4 Gross organic N processes**

172 One day before starting the pool dilution experiment FAA concentrations were determined in an aliquot of pre-  
173 incubated soil. The isotope pool dilution experiment and sample analyses were conducted as described previously by  
174 Noll et al. (2019a). In brief, 4 g of soil were weighed into transparent HDPE vials in duplicates and 400 µl of a <sup>15</sup>N  
175 tracer solution were added drop wise. Samples were shaken vigorously to guarantee good mixing of the tracer. The  
176 tracer solution was prepared from a highly <sup>15</sup>N enriched amino acid mixture (U-15N-98 at% <sup>15</sup>N amino acid mixture  
177 from crude algal protein, Cambridge Isotope Laboratories, Radeberg, Germany). The total amount of added <sup>15</sup>N was  
178 adjusted to about 20% of the native FAA pool. The incubation was terminated after 15 and 45 min by addition of  
179 cold KCl (4 °C) and samples were extracted for 1 h on a rotary shaker and filtered at 4 °C. Prior to measuring the  
180 isotopic composition of FAA NH<sub>4</sub><sup>+</sup> was removed by microdiffusion (Lachouani et al., 2010; Noll et al., 2019a).  
181 Extracts were microdiffused for 48 h. To measure the concentration and atom %<sup>15</sup>N of FAA 2 ml of pre-treated  
182 extracts were transferred into 12 mL glass exetainers and the α-amino group was cleaved/oxidized by NaClO and  
183 KBr as catalyst under alkaline conditions as described by Zhang and Altabet (2008) and modified by Noll et al.  
184 (2019a). Subsequently the produced NO<sub>2</sub><sup>-</sup> was converted to N<sub>2</sub>O by buffered NaN<sub>3</sub> (NaN<sub>3</sub> in 100% acetic acid 1:1).  
185 The produced N<sub>2</sub>O was measured with a purge-and-trap isotope ratio mass spectrometer (PT-IRMS) consisting of a  
186 Finnigan Delta V Advantage IRMS (Thermo Fisher, Germany) and a Gasbench II headspace analyzer (Thermo

187 Fisher, Germany) with cryo-focusing unit. Calibration was done according to Lachouani et al. (2010) and Noll et al.  
188 (2019a)

## 189 2.5 Data analyses and statistics

190 Gross rates of protein depolymerization (GP) and microbial amino acid uptake (GU) were calculated according to  
191 Kirkham and Bartolomew (1954) and Wanek et al. (2010):

$$GP = \frac{(N_{t2} - N_{t1})}{(t2 - t1)} * \frac{\text{LN} \left[ \frac{(at\%^{15}N_{t1} - at\%^{15}N_b)}{(at\%^{15}N_{t2} - at\%^{15}N_b)} \right]}{\text{LN} \left( \frac{N_{t2}}{N_{t1}} \right)}$$

192

$$GU = \frac{(N_{t1} - N_{t2})}{(t2 - t1)} * \left( 1 + \frac{\text{LN} \left[ \frac{(at\%^{15}N_{t2} - at\%^{15}N_b)}{(at\%^{15}N_{t1} - at\%^{15}N_b)} \right]}{\text{LN} \left( \frac{N_{t2}}{N_{t1}} \right)} \right)$$

193 where  $N_{t1}$  and  $N_{t2}$  are the concentrations of FAA-N at the time points  $t1$  (15 min) and  $t2$  (45min).  $^{15}\text{N}$  content in  
194 amino acids at the time points of termination are expressed as  $at\%^{15}\text{N}_{t1}$  and  $at\%^{15}\text{N}_{t2}$ , while  $at\%^{15}\text{N}_b$  is the  
195 background  $^{15}\text{N}$  abundance (0.366  $at\%^{15}\text{N}$ ) in non-labeled samples. Mean residence times of FAA were estimated as  
196 free amino acid pool size divided by microbial amino acid uptake rate. Microbial C:N and N:P imbalances were  
197 calculated as the ratio of resource C:N or N:P over microbial C:N or N:P.

198 For statistical analyses of single variables, mineral soils were grouped by bedrock (limestone, sediments, silicates) or  
199 by land use (cropland, grassland, woodlands). Prior to statistical analyses data were checked for normality and  
200 transformed if necessary. Land use effects on process rates and soil properties were analyzed for the 22 sites where  
201 cropland, grassland and woodland soils could be sampled in close vicinity (66 data points). Since only one  
202 composite sample was analyzed per land use at each site and therefore single observations were not independent,  
203 'site' was included as factor in a two-way ANOVA to account for differences between sites (climate, bedrock, soil  
204 type). Given the low (non-significant) land use effects across sites the effects of bedrock were analyzed by one-way  
205 analysis of variance (ANOVA) followed by Tukey HSD tests. Not accounting for land use here allowed to analyze  
206 the whole data set (n=91) instead of restricting this to the 22 site data set (n=66). Differences in process rates and soil  
207 properties between organic and underlying mineral soil horizons were analyzed by paired t-tests for the 13 sites  
208 where organic and mineral horizons were sampled. Linear mixed models were used to explore the effect of soil  
209 properties and climate on protein depolymerization rates with land use as random factor. The most parsimonious  
210 model was selected by Akaike's information criterion (AIC). Multicollinearity was assessed by variance inflation  
211 factors (VIF). Variables with VIF larger than 2.5 were excluded from the model. Partial correlations were used to  
212 control for the effect of soil geochemical properties on the relationship between climate and the response variables  
213 (i.e. protein depolymerization rates, leucine-amino peptidase activity and NaOH-extractable protein; Doetterl et al.,  
214 2015; Luo et al., 2011). Significant changes of the correlation coefficient were assumed when the 95% confidence  
215 interval of the zero-order correlation and the partial correlation did not overlap. Partial correlations were analyzed  
216 using 'ppcor' in R environment (Kim, 2015). Effects of climate parameters and their interactions on process rates

217 were assessed by linear mixed effect models with soil parent material or land use as random effects. We used  
218 structural equation modelling (SEM) to explore direct and indirect effects of climate, geology and soil properties on  
219 protein depolymerization rates. We used parameters which correlated significantly with protein depolymerization to  
220 construct a base model for gross protein depolymerization rates. Input variables were tested for multivariate  
221 normality and linearity. If necessary variables were log transformed to mitigate departure from model assumptions.  
222 The model was then analyzed using the ‘lavaan’ package (Rosseel, 2018) in R. Model fit was evaluated using Chi-  
223 square statistics ( $p > 0.05$ ). The most parsimonious model was identified by step-wise deletion of non-significant  
224 paths. Akaike’s information criterion (AIC) was used to compare competing model fits. We followed the two-index  
225 strategy proposed by Hu and Bentler (1999) to describe the specified model and the data covariance-matrix and  
226 reported root mean square error of approximation (RMSEA) and standardized root mean square residual (SRMR).  
227 Good model-data fit is indicated by  $RMSEA \leq 0.06$  and  $SRMR \leq 0.08$ . All statistics were performed in R 3.1.3 (R  
228 Development Core Team, 2008). Direct and indirect effect sizes in path analysis were assessed by ‘lavaan’, indirect  
229 effects being calculated by multiplying the (direct) path effects that constitute the effect.

## 230 **3 Results**

### 231 **3.1 Effects of bedrock, land use, soil horizon and climate**

232 Protein depolymerization rates were strongly related to soil physicochemical properties like soil pH,  
233 amorphous Fe and Al minerals ( $Fe_{\text{oxalate}}$ ,  $Al_{\text{oxalate}}$ ) as well as to soil organic matter ( $C_{\text{org}}$ , total N), NaOH-extractable  
234 protein and microbial biomass ( $C_{\text{mic}}$ , PLFA) (Figure 3, Table S3). NaOH-extractable protein content increased with  
235 SOC, soil TN, root biomass and amorphous Fe- and Al-(hydr)oxides (Table S3, Figure 3). Soil pH was negatively  
236 correlated with gross depolymerization and NaOH-extractable protein, but positively to peptidase activity (Figure 3).  
237 However, across all sites as well as within subgroups we found no significant (putatively positive) correlation  
238 between aminopeptidase activity, a wide spread soil proteolytic enzyme, and protein depolymerization rates (Figure  
239 S5). In order to further examine the potential edaphic controls on gross protein depolymerization in mineral soils as  
240 well as interaction effects with land use we used multiple linear regression analyses. In the most parsimonious model  
241 NaOH-extractable protein explained 37% of the variance, emphasizing the prominent role of substrate availability  
242 controlling depolymerization rates (Figure 2). Land use did not interact with specific edaphic properties, and linear  
243 mixed effect models with land use as random factor confirmed the suggested main controls on depolymerization  
244 rates, i.e. protein availability and soil pH (Table S4).

245 Climate effects on depolymerization rates were analyzed by linear regression analyses including climate  
246 parameters, land use and interaction effects. We found significant effects of mean annual temperature (MAT) and  
247 mean annual precipitation (MAP) and of their interaction (MAP:MAT) (Table S5). Land use had no significant effect  
248 on the climate response of protein depolymerization, as shown by similar negative correlations between  
249 depolymerization and MAT in all three land use types (Figure 4). The model explained about 42% of the variance.  
250 Although the climatic humidity index (MAP:PET), expressed as MAP over potential evapotranspiration (PET), was  
251 not included in the most parsimonious model, the strong logarithmic increase of depolymerization rates with climatic  
252 humidity ( $r^2 = 0.632$ ,  $p < 0.001$ ) across all sites and land use types was striking (Figure 4). The most parsimonious



253 linear mixed effect model included land use as random factor and showed a strong negative effect of MAT and a  
 254 positive effect of MAP. The model explained about 47% of the variance in protein depolymerization  
 255

### 256 3.2 Integrated effects of edaphic properties and climate

257 Since soil parent material, which is a main driver of soil geochemical properties, is not uniformly distributed across  
 258 the sampled transect, climate effects (MAT and MAP) on gross protein depolymerization rates, leucine-amino  
 259 peptidase activity and NaOH-extractable protein were analysed by partial regression analyses controlling for  
 260 geochemical parameters (Figure 4). For instance we found a negative zero-order correlation between protein  
 261 depolymerization and MAT ( $r = -0.63$ ,  $p < 0.01$ ), the correlation coefficient decreasing significantly when removing

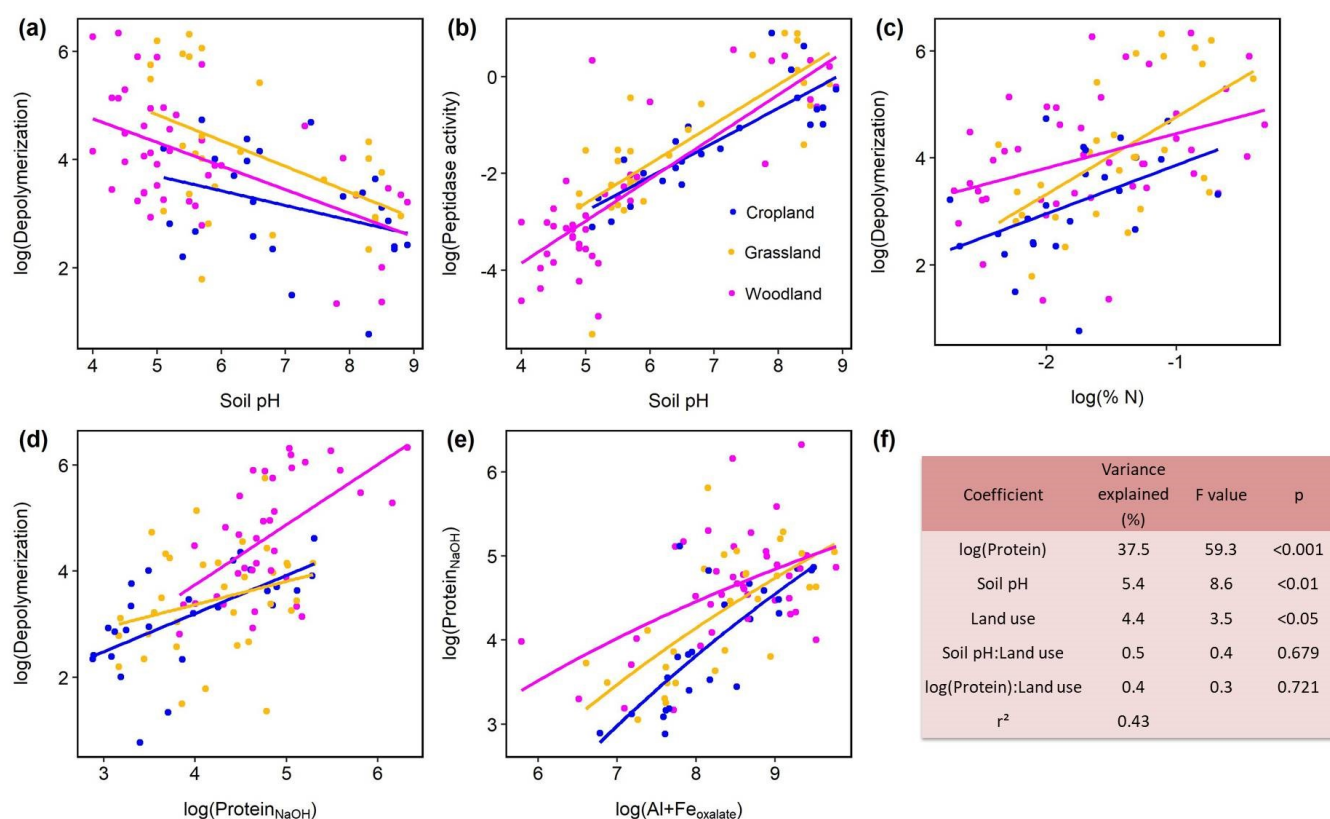


**Figure 3** Effects of soil properties on gross protein depolymerization rates in mineral soils. Relationship of pH and (a), log(Protein depolymerization) and (b), log(leucine-amino peptidase activity). (c), Relationship of soil total N and protein depolymerization rate (d), Relationship of NaOH-extractable protein and protein depolymerization rate. Color codes indicate land use type. (e), Relationship of oxalate extractable Al and Fe and NaOH-extractable protein. (f), Analyses of variance of the most parsimonious linear regression model of log(gross protein depolymerization rate) explained by soil properties, land use and their interaction effects ( $n = 95$ ). Total model fit is given as adjusted  $r^2$ .

262 correlations with Al, Fe or the sum of oxalate-extractable Fe and Al (Figure 4). NaOH-extractable protein was  
263 negatively correlated to MAT ( $r = -0.53$ ,  $p < 0.01$ ), the correlation coefficient decreasing significantly by removing  
264 the correlations with Al and the sum of oxalate extractable Al and Fe. All zero-order correlations with MAT  
265 decreased significantly after removing the effects of soil geochemical parameters. Mean annual precipitation was  
266 weakly positively correlated with protein depolymerization ( $r = 0.29$ ,  $p < 0.05$ ) and NaOH-extractable protein ( $r =$   
267  $0.46$ ,  $p < 0.01$ ), however, the removal of correlations with geochemical parameters having no significant effect.

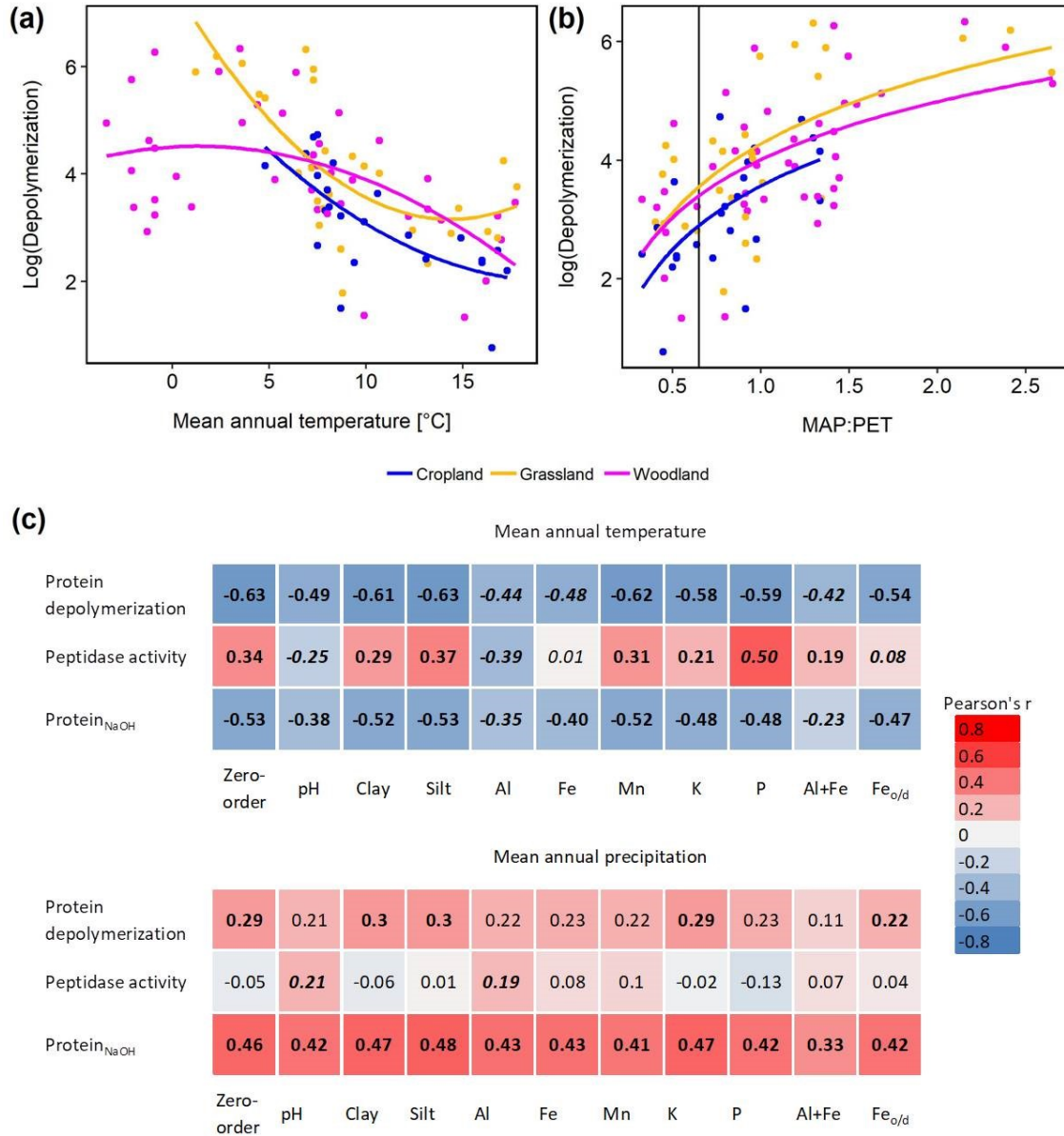


**Figure 4** Climate effects on gross protein depolymerization. (a), Relationship between the natural logarithm of gross protein depolymerization and 2nd polynomial regression fit for cropland (adjusted  $r^2 = 0.455$ ,  $p < 0.001$ ,  $n = 24$ ), grassland ( $r^2 = 0.480$ ,  $p < 0.001$ ,  $n = 28$ ) and woodland ( $r^2 = 0.219$ ,  $p < 0.01$ ,  $n = 48$ ) soils. (b), Relationship between the natural logarithm of gross protein depolymerization rates and the ratio of mean annual precipitation over potential evapotranspiration (MAP:PET) and regression fit ( $y = \log(x)$ ) for cropland (adjusted  $r^2 = 0.330$ ,  $p < 0.01$ ,  $n = 24$ ), grassland (adjusted  $r^2 = 0.371$ ,  $p < 0.001$ ,  $n = 28$ ) and woodland (adjusted  $r^2 = 0.318$ ,  $p < 0.001$ ,  $n = 48$ ) soils. The vertical line indicates the transition from arid to humid climate conditions (MAP:PET = 0.65). (c), zero-order and partial correlations (Pearson's  $r$ ) between climate variables (MAT and MAP) and organic N cycling (protein depolymerization rate, leucine-amino peptidase activity and Protein<sub>NaOH</sub>) controlled for geochemical variables. Significant correlations are indicated by bold numbers. Significant changes of the correlation coefficients compared to the zero-order correlation are indicated by italic numbers.

269 **3.3 Path analyses**

270 The a priori model was constructed according to the hypothesis illustrated in Figure 1. After removing insignificant  
 271 paths the model contained NaOH-extractable protein, soil pH, amorphous Fe and Al, and MAP ( $X^2 = 2.49$ ,  $p =$   
 272  $0.288$ ;  $RMSEA = 0.048$ ,  $SRMR = 0.023$ ). The revised model explained 43% of the variance in gross protein  
 273 depolymerization and 49% of the variance in NaOH-extractable protein. Protein depolymerization in mineral soils  
 274 was highly dependent on NaOH-extractable protein. Soil pH had direct and indirect (via NaOH-extractable protein)  
 275 negative effects on depolymerization rates (Figure 5). MAP and amorphous Fe and Al had positive effects on NaOH-  
 276 extractable protein and thereby positive indirect effects on protein depolymerization. The total effects (direct effects  
 277 + indirect effects) of the model parameters on protein depolymerization increased in the order amorphous Fe and  
 278  $Al < soil\ pH < MAP < NaOH\text{-extractable\ protein}$ .

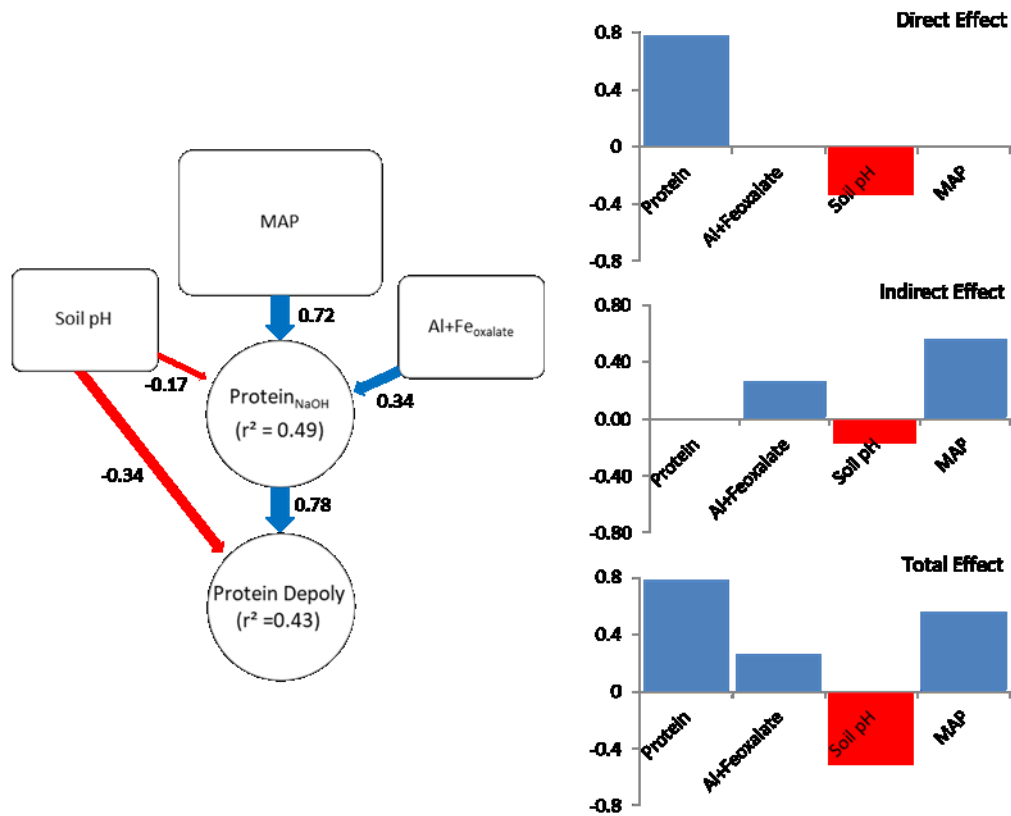


Figure 5 Direct and indirect effects in gross protein depolymerization rates. Controls of Path analyses for gross protein depolymerization rates in mineral soils and coefficients for direct, indirect and total effects (n=91). Significant effects ( $p < 0.05$ ) are indicated by red (negative) and blue (positive) arrows. Effect sizes are indicated by line width. Numbers beside arrows indicate the standardized parameter estimates. Numbers within boxes indicate the variance explained by the model.

279

## 280 **4 Discussion**

### 281 **4.1 Land use and soil horizon effects on protein depolymerization**

282 Our results revealed, that land use, which is an important driver of SOM contents and soil microbial community  
283 composition (Lauber et al., 2008; Jangid et al., 2008) and consequently of the set of excreted proteolytic enzymes,  
284 might only exert a minor control on soil organic N cycling at large spatial scales. Though effects were significant for  
285 individual sampling sites (Table S2), land use had no significant effect on the response of protein depolymerization  
286 rates to soil properties, explaining less than 5 % of the total variation in multiple linear regression models (Figure 3,  
287 Table S5). This demonstrates that the same drivers operated on protein depolymerization in croplands, grasslands  
288 and woodlands, and triggering the same directional and strength of response across land uses. Effects of land use  
289 were therefore likely strongly overprinted by large scale changes in climate and geology, since in the applied  
290 sampling scheme the factor land use was nested in large scale climatic and geological controls across a continental  
291 transect. Effects of land use might be more prominent at a smaller regional to local scale (Noll et al. 2019b), which  
292 was, however, not accessible with this data set.

293 At the continental level, gross protein depolymerization rates increased with soil organic matter (SOM), from  
294 Mediterranean to temperate and boreal ecosystems. Though vegetation N limitation increases with latitude (Kang et  
295 al, 2010, Du et al., 2020; Augusto et al., 2017), rising depolymerization rates with latitude indicate increasing labile  
296 organic N provisioning to microbes and plants at higher latitudes under lab conditions. This positive effect of  
297 substrate availability on depolymerization rates was further confirmed by high gross protein depolymerization rates  
298 observed in organic horizons in boreal and alpine biomes, which significantly exceeded those in the underlying  
299 mineral soils (Table S2). However, in contrast to findings of Mooshammer et al. (2012) for decomposing litter, our  
300 data revealed no indication that resource C:N or microbial C:N imbalances affected protein depolymerization rates in  
301 organic soils and thereby highlights the differential element viz. nutrient limitation of plants and soil microbes across  
302 large spatial scales as proposed by Capek et al. (2018).

303

### 304 **4.2 Substrate limitation of protein depolymerization is controlled by organo-mineral interactions**

305 Across all land use types NaOH-extractable protein and soil pH were the main predictors for gross protein  
306 depolymerization in mineral soils, indicating that soil properties that determine protein availability such as texture,  
307 mineral assemblage or soil pH need to be considered when addressing large-scale controls of soil organic N cycling.  
308 Gross protein depolymerization was lower in soils developed on limestone than in soils developed on sediments or  
309 silicates, which is emphasized by the inverse relationship between depolymerization rates and soil pH (Figure 3).  
310 Moreover, depolymerization rates decreased with increasing clay content. Proteins can be adsorbed to clay surfaces  
311 by electrostatic interactions between positively charged amino acid side chains and siloxane surfaces of clay minerals  
312 (Staunton and Quiquampoix, 1994; Quiquampoix and Ratcliffe, 1992). Sorption experiments in artificial soils  
313 showed that at neutral soil pH (>7) clay minerals are the main sorption sites for organic N (Pronk et al., 2013). This  
314 can be further enhanced by polyvalent cations as  $\text{Ca}^{2+}$  or  $\text{Mg}^{2+}$ , which can bridge the negative charges of clay  
315 mineral surfaces and proteins (Cao et al., 2011; Lützow et al., 2006). Aside from the stabilization on mineral

316 surfaces, high clay contents, as found in limestone soils, promote soil aggregation and thereby the occlusion of  
317 organic matter and proteins rendering them inaccessible for enzymatic attack (Lützw et al., 2006). In contrast Fe-  
318 and Al- oxyhydroxides, the main sorption sites for SOM at acidic pH, were positively correlated to gross  
319 depolymerization rates. SOM accumulation is usually higher in acidic soils due to ligand exchange between  
320 protonated hydroxyl groups of Fe- and Al- minerals and carboxyl groups of organic molecules (Gu et al., 1994;  
321 Kleber et al., 2005; Kaiser and Guggenberger, 2000). Therefore the overall organic N pool size is expected to be  
322 larger in fine textured soils and in soils high in Fe- and Al-oxyhydroxides. Moreover, the strength of the binding  
323 interaction between Fe- and Al-oxyhydroxides and SOM, and more specifically with organic N including proteins, is  
324 higher by 50% than with typical clay minerals (Newcomb et al, 2017). Consequently soils rich in Fe- and Al-  
325 oxyhydroxides contain larger pools of proteolytic substrates (organic N and proteins), but these substrates can be  
326 more strongly bound and therefore be less accessible for microbial utilization. However, column experiments with  
327 embedded goethite in acidic soils revealed that sufficiently large amounts of stabilized OM can be re-dissolved by  
328 progressing percolation of dissolved OM and the subsequent exchange with adsorbed compounds such as peptides  
329 (Leinemann et al., 2018), which thereby become available for enzymatic attack and/or microbial utilization. The  
330 bioavailability of oxide-bound organic N is further supported by the strong positive correlation between NaOH-  
331 extractable protein and amorphous Fe- and Al-oxyhydroxides (Table S3), since NaOH mainly extracts loosely bound  
332 proteins (Wattel-Koekkoek et al., 2001). Overall, Fe- and Al-oxyhydroxides remained as a significant parameter in  
333 linear models and path analyses and should therefore be considered as important predictors for the potential of a soil  
334 to retain and accumulate SOM (Moni et al, 2007; Fang et al., 2019), which promotes microbial biomass and activity  
335 (Xu et al., 2013; Hartman and Richardson, 2013). The positive effect of the potential to accumulate SOM can be  
336 attributed to the continuous exchange of adsorbed compounds and the consequent steady release of organic N. The  
337 net effect of these adverse interactions is currently unknown; therefore this study is among the first to show a net  
338 positive effect of Fe- and Al oxyhydroxides on the *in situ* rates of depolymerization of high molecular weight-ON  
339 substrates.

340 Though the total N pool size was not significantly different between soils developed on the three bedrock  
341 types, NaOH-extractable protein increased on the order limestone<sediment<silicate. NaOH-extractable protein  
342 accounted for  $4.4 \pm 1.7\%$  of total N in sediment soils and for  $6.4 \pm 3\%$  in silicate soils, compared to  $2.9 \pm 2\%$  in  
343 limestone soils. This could be either attributed to a lower extraction efficiency of proteins with 0.5 M NaOH from  
344 clay minerals at high soil pH or to an increase of non-hydrolysable organic N. The studied limestone soils were  
345 characterized by higher amounts of crystalline iron ( $\text{Fe}_{d-o}$ ), namely hematite, which forms almost irreversible  
346 interactions with SOM (Gu et al., 1995), even at high soil pH, due to formation of coordination complexes between  
347 carboxyl groups and Fe atoms (Koutsoukos et al., 1983; Quiquampoix, 2000). The formation of strong peptide  
348 complexes with crystalline Fe minerals is also supported by findings of Mikutta et al. (2010), who showed an  
349 increase of non-hydrolysable peptide-N with the proportion of crystalline Fe minerals across a soil chronosequence.

350 From linear regression and path analyses soil pH was revealed as the second most important predictor of  
351 gross protein depolymerization rates. Soil pH mirrors the strength of  $\text{Ca}^{2+}$ -bridging of negatively charged ligands (as  
352 protein-carboxylates) to negatively charged soil particles (clays), but also the weathering status of soils, which comes  
353 with the formation of secondary clays and Fe- and Al-oxyhydroxides. However, soil pH also directly affects

354 electrostatic interactions between mineral surfaces and proteins. Sorption of proteins on clay and Fe-mineral surfaces  
355 is usually highest close to the isoelectric point of a specific protein. Due to the complex nature of proteins including  
356 different functional groups and tertiary structures isoelectric points range from pH 1 for pepsin to pH 11 for  
357 lysozyme, making predictions for soil proteins at large impossible. Sorption of bovine and human serum albumin on  
358 montmorillonite peaked at pH ~5, whereas adsorption of cytochrome c or ribonuclease on hematite peaked at pH 8 to  
359 10, all being close to their isoelectric points (Khare et al., 2006; Koutsoukos et al., 1983; Quiquampoix and Ratcliffe,  
360 1992).

361           However, the negative effect of soil pH on gross depolymerization is in sharp contrast to the increase of  
362 peptidase activity with soil pH. To allow comparisons between enzyme activities and depolymerization rates,  
363 enzyme activities were measured (i) in unbuffered soil slurries at natural soil pH and (ii) compared to enzyme  
364 activities measured at the same pH in acetate buffer (pH 5.2). Hence, unbuffered peptidase activities were highest in  
365 limestone soils close to the pH optima of proteolytic enzymes at about 8 (Sinsabaugh et al., 2008) (Figure S5). The  
366 lack of correlation between gross depolymerization and peptidase activity, but rather the maximum of protein  
367 depolymerization coinciding with the minima of potential protease activity, implies that gross protein  
368 depolymerization rates are rather substrate limited than enzyme limited. It further highlights that differences in  
369 protein depolymerization between alkaline, neutral and acidic soils are due to changes in substrate (protein)  
370 availability rather than due to changes in microbial community structure and enzymatic activity. Even when  
371 peptidase was measured at the same pH, potential peptidase activity was higher in limestone soils compared to  
372 sediment and silicate soils (Table S2, Figure S6), which implies enhanced microbial enzyme excretion in limestone  
373 soils in response to lower protein availability.

374 The generally low protein depolymerization rates in limestone soils are in accordance to our previous findings from  
375 soils developed on limestone and silicate bedrock in Austria (Noll et al., 2019b), demonstrating that soil parent  
376 material pre-determines depolymerization rates on regional and continental scales. We assume that in limestone soils  
377 proteins are strongly stabilized on phyllosilicates and crystalline Fe-oxides or occluded within soil aggregates  
378 rendering them inaccessible for proteolytic attack. Soil microorganisms respond to this N-limitation by greater  
379 investments into the production and excretion of extracellular enzymes mining for these soil organic N forms (Chen  
380 et al., 2014), as shown by the enhanced potential activities of amino peptidase in limestone soils.

### 381 **4.3 Climate drives protein depolymerization by affecting mineral weathering and plant productivity**

382 Climate is a major control on mineral weathering and net primary productivity (Norton et al., 2014; Doetterl et al.,  
383 2015) and thereby affects protein stabilization and input of fresh OM by plants. Across the studied climate transect  
384 gross protein depolymerization rates decreased with MAT and increased with MAP, respectively increased with the  
385 climatic humidity index (MAP:PET). As demonstrated by the partial correlations, part of the negative effect of MAT  
386 on depolymerization rates can be explained by concomitant changes in amorphous Al- and Fe-oxyhydroxides and  
387 soil pH, which affect protein availability (Figure 4). The correlation coefficient between MAT and depolymerization  
388 significantly decreased by removing the effects of soil Fe- and Al-oxyhydroxides, while the decrease by removing  
389 effects of soil pH was not significant. The important role of soil geochemical properties on protein stabilization is  
390 underpinned by the even stronger effect of soil properties on the relation between MAT and NaOH-extractable

391 protein (Figure 4). In the Mediterranean region limestone-derived red soils are predominant. The so called “Terra  
392 Rossa” soils are characterized by high soil pH, high clay contents and relatively high amounts of crystalline Fe as  
393 well as a low  $\text{Fe}_{\text{oxalate}}:\text{Fe}_{\text{dithionite}}$  ratio, caused by the preferential formation of the Fe-oxide hematite over the Fe-  
394 hydroxide goethite during the summer dry period (Yaalon, 1997). As described above, these specific soil properties  
395 might foster stabilization of proteins and thereby constrain gross protein depolymerization. Under more humid  
396 conditions soil pH drops due to leaching of base cations (e.g.  $\text{Ca}^{2+}$ ) and more intensive chemical weathering  
397 promotes the formation of higher amounts of charged mineral surfaces as amorphous Fe- and Al oxyhydroxides  
398 (Doetterl et al., 2015). This increase in soil acidification at higher latitude is further facilitated by the predominance  
399 of silicate bedrocks in Northern Europe. Although MAP is an important driver of soil weathering and thereby affects  
400 soil pH and the formation of charged mineral surfaces, the positive effect of MAP on depolymerization rates and  
401 proteins was not significantly biased by soil properties in the partial correlations (Figure 4). However, the weak  
402 effects of Fe and Al oxyhydroxides on the relation between protein depolymerization and MAP, or between NaOH-  
403 extractable protein and MAP, might indicate the role of MAP in soil mineral formation during pedogenesis.  
404 Particularly in arid and sub-arid biomes precipitation determines plant net primary production (Yang et al., 2008; Del  
405 Grosso et al., 2008) and thereby the input of fresh organic matter into the soil. This might further explain the strong  
406 relationship between NaOH-extractable protein and MAP, as indicated by linear models and path analyses and is  
407 further supported by the proximate increase in depolymerization with the climatic humidity index (Figure 4). The  
408 logarithmic response implies that the limiting effect of MAP is stronger under sub-arid conditions, which is in  
409 accordance to findings showing that in water limited regions NPP is strongly controlled by MAP (Yang et al., 2008).  
410 Therefore, we conclude that, in sub-arid regions in Southern Europe precipitation constrains plant biomass  
411 production and consequently OM input into soils. In contrast, our results reveal that the increase of gross  
412 depolymerization with MAT is biased by ‘concurrent’ changes in soil parent material across the studied transect,  
413 while MAP likely controls net primary productivity and mineral weathering (Gislason et al., 2009; La Pierre et al.,  
414 2016). Both, partial correlations and path analyses support our hypothesis that climate is a rather indirect driver of  
415 soil organic N cycling by its effects on soil chemical weathering and more specifically the formation of specific  
416 minerals and consequently on soil organic matter accumulation.

417 Path analysis emphasized the important role of climate and bedrock as pre-determinants of OM stabilization  
418 and protein availability, and suggested that MAP, soil pH, and Fe- and Al-oxyhydroxides are indirect controls on  
419 gross protein depolymerization, which is mediated by protein availability, while soil pH and NaOH-extractable  
420 protein are direct controls on gross protein depolymerization. The indirect effect of MAP exceeded the direct effects  
421 of soil mineralogy and pH. However, NaOH-extractable protein overall was the main predictor of protein  
422 depolymerization rates. The negative direct effect of soil pH on depolymerization rates is explained by the low  
423 solubility of proteins at high soil pH (Franco and Pessôa Filho, 2011), which restricts diffusion throughout the soil  
424 matrix and limits the accessibility of protein substrates to enzymatic attack. In contrast, the negative pH effect on  
425 NaOH-extractable protein is attributed to the accumulation of SOM at acidic soil pH and the increased interactions  
426 with Fe- and Al-oxyhydroxides (Kaiser and Guggenberger, 2003; Gu et al., 1994). With increasing soil pH amino  
427 groups of proteins become de-protonated and thereby proteins become negatively charged, which increases the  
428 repulsion from negatively charged mineral surfaces and decreases the adsorption to Fe-oxides and phyllosilicates



429 (Cao et al., 2011). Furthermore, soil pH, texture and mineral assemblage are drivers of microbial community  
430 composition and affect the availability of other nutrients like P or K (Fierer and Jackson, 2006; Lauber et al., 2008).  
431 Neither  $\text{Ca}^{2+}$  nor clay was included in the final model, despite their important role in stabilizing soil organic matter  
432 (Lützow et al., 2006). We assume that the effects of  $\text{Ca}^{2+}$  and clay are outweighed by effects of soil pH and MAP.  
433 Soil pH decreased from clay-rich limestone soils to sediment soils and to more sandy silicate soils, and thereby co-  
434 varied with  $\text{Ca}^{2+}$  and clay content, while MAP regulates mineral dissolution and leaching of  $\text{Ca}^{2+}$  (Gislason et al.,  
435 2009). Land use was non-significant and therefore was removed from the revised path model, which is in accordance  
436 to results from general linear models, showing that soil properties and climate variables explained the greatest  
437 percentage of the variance in gross protein depolymerization. Although path analyses provided an integrative model  
438 of controls driving gross protein depolymerization, it offered an incomplete picture. In this study we focused on the  
439 large scale patterns, which explained more than 40% of the variation in organic N cycling. However, regional or  
440 local effects, such as by topography, land use history, land use intensity, and plant community composition were not  
441 accessible with this data set, but are likely important controls on organic N cycling at regional spatial scales.

## 442 **5 Conclusions**

443 Our results highlight the important role of soil geochemistry when estimating microbial nutrient cycling on  
444 continental to global scales, and demonstrate that at this scale soil parent material and climate override the effects of  
445 land use on soil organic N transformations.. The amount of NaOH-extractable protein was here identified as the most  
446 important direct predictor of protein depolymerization rates, while peptidase activity negatively related to protein  
447 depolymerization, and therefore rather reflects a proxy of microbial N limitation according to enzyme allocation  
448 theory (Allison et al., 2010). Since protein availability and thereby protein depolymerization is strongly constrained  
449 by soil organic matter-mineral interactions, shifts in climate (precipitation regime) and associated alterations in soil  
450 weathering should be considered as drivers of ecosystem N availability with strong repercussions on ecosystem C  
451 cycle processes. This also needs to be validated in large-scale coupled climate-biogeochemistry and in Earth system  
452 models to help predict and mitigate global change effects.

## 453 **Data availability**

454 All data and codes presented in this paper are available at DRYAD, <https://datadryad.org/stash>.

## 455 **Author contribution**

456 **LN wrote the paper, conducted fieldwork and laboratory work, analyzed and interpreted the data. SZ, QZ**  
457 **and YH conducted laboratory work, analyzed the data and edited the paper. FH analyzed the data and edited**  
458 **the paper. WW designed the study, interpreted the data and edited the paper.**

459 Competing interests

460 The authors declare that they have no competing interests.

461 Acknowledgements

462 We thank Theresa Böckle, Daniel Wasner, Vsevolods Girsovics and Rebecca Lieske for soil sampling and assistance  
463 in the lab. We would like to thank Jukka Pumpanen for providing soil samples from the Värriö District Nature  
464 Reserve. This project was funded by the Austrian Science Fund (FWF, Project P-28037-B22).

## 465 References

- 466 Adamczyk, B., Kitunen, V., and Smolander, A.: Polyphenol oxidase, tannase and proteolytic activity in relation to tannin  
467 concentration in the soil organic horizon under silver birch and Norway spruce, *Soil Biology and Biochemistry*, 41, 2085-2093,  
468 <https://doi.org/10.1016/j.soilbio.2009.07.018>, 2009.
- 469 Allison, S. D., Weintraub, M. N., Gartner, T. B., and Waldrop, M. P.: Evolutionary-economic principles as regulators of soil  
470 enzyme production and ecosystem function. in: *Soil enzymology*, Springer, Berlin, Heidelberg, Germany, 229 - 243, 2010.
- 471 Angst, G., Messinger, J., Greiner, M., Häusler, W., Hertel, D., Kirfel, K., Kögel-Knabner, I., Leuschner, C., Rethemeyer, J., and  
472 Mueller, C. W.: Soil organic carbon stocks in topsoil and subsoil controlled by parent material, carbon input in the rhizosphere,  
473 and microbial-derived compounds, *Soil Biology and Biochemistry*, 122, 19-30, <https://doi.org/10.1016/j.soilbio.2018.03.026>,  
474 2018.
- 475 Asch, K.: IGME 5000: 1: 5 Million international geological map of Europe and Adjacent Areas—final version for the internet.  
476 BGR, Hannover, 2005.
- 477 Augusto, L., Achat, D. L., Jonard, M., Vidal, D., and Ringeval, B.: Soil parent material—A major driver of plant nutrient  
478 limitations in terrestrial ecosystems, *Global Change Biology*, 23 9, 3808-3824, 2017.
- 479 BGR [Bundesanstalt für Geowissenschaften und Rohstoffe]: Soil Regions Map of the European Union and Adjacent Countries  
480 1:5000000 (Version 2.0), Special Publication Ispra. EU catalogue number S.P.I.05.134., 2005.
- 481 Bohn, U. and Katenina, G.: Karte der natürlichen Vegetation Europas [: Map of the natural vegetation of Europe, Bundesamt für  
482 Naturschutz2000.
- 483 Brookes, P., Landman, A., Pruden, G., and Jenkinson, D.: Chloroform fumigation and the release of soil nitrogen: a rapid direct  
484 extraction method to measure microbial biomass nitrogen in soil, *Soil biology and biochemistry*, 17, 837-842, 1985.
- 485 Callesen, I., Raulund-Rasmussen, K., Westman, C. J., and Tau-Strand, L.: Nitrogen pools and C : N ratios in well-drained Nordic  
486 forest soils related to climate and soil texture, *Boreal Environment Research*, 12, 681-692, 2007.
- 487 Cao, Y., Wei, X., Cai, P., Huang, Q., Rong, X., and Liang, W.: Preferential adsorption of extracellular polymeric substances from  
488 bacteria on clay minerals and iron oxide, *Colloids and Surfaces B: Biointerfaces*, 83, 122-127,  
489 <https://doi.org/10.1016/j.colsurfb.2010.11.018>, 2011.
- 490 Capek, P. T., Manzoni, S., Kastovska, E., Wild, B., Diakova, K., Barta, J., Schneckner, J., Blasi, C., Martikainen, P. J., Alves, R. J.  
491 E., Guggenberger, G., Gentsch, N., Hugelius, G., Palmtag, J., Mikutta, R., Shibistova, O., Urich, T., Schleper, C., Richter, A., and  
492 Santruckova, H.: A plant-microbe interaction framework explaining nutrient effects on primary production, *Nature Ecology &  
493 Evolution*, 2, 1588-1596, 10.1038/s41559-018-0662-8, 2018.
- 494 Chen, R., Senbayram, M., Blagodatsky, S., Myachina, O., Dittert, K., Lin, X., Blagodatskaya, E., and Kuzyakov, Y.: Soil C and N  
495 availability determine the priming effect: microbial N mining and stoichiometric decomposition theories, *Global change biology*,  
496 20, 2356-2367, 2014.
- 497 Chen, Q., Yang, F., & Cheng, X.: Effects of land use change type on soil microbial attributes and their controls: Data synthesis,  
498 *Ecological Indicators*, 138, 108852, 2022.
- 499 De Vries, F. T., Hoffland, E., van Eekeren, N., Brussaard, L., and Bloem, J.: Fungal/bacterial ratios in grasslands with contrasting  
500 nitrogen management, *Soil Biology and Biochemistry*, 38, 2092-2103, 2006.
- 501 Del Grosso, S., Parton, W., Stohlgren, T., Zheng, D., Bachelet, D., Prince, S., Hibbard, K., and Olson, R.: Global potential net  
502 primary production predicted from vegetation class, precipitation, and temperature, *Ecology*, 89, 2117-2126, 2008.
- 503 Delgado-Baquerizo, M., Maestre, F. T., Gallardo, A., Bowker, M. A., Wallenstein, M. D., Quero, J. L., Ochoa, V., Gozalo, B.,  
504 García-Gómez, M., and Soliveres, S.: Decoupling of soil nutrient cycles as a function of aridity in global drylands, *Nature*, 502,  
505 672, 2013.
- 506 Doetterl, S., Stevens, A., Six, J., Merckx, R., Van Oost, K., Pinto, M., Casanova-Katny, A., Munoz, C., Boudin, M., Venegas, E.,  
507 and Boeckx, P.: Soil carbon storage controlled by interactions between geochemistry and climate, *Nature Geoscience*, 8, 780-+,  
508 10.1038/NNGEO2516, 2015.
- 509 Du, E., Terrer, C., Pellegrini, A. F., Ahlström, A., van Lissa, C. J., Zhao, X., Xia, N., Wu., X. and Jackson, R. B.: Global patterns  
510 of terrestrial nitrogen and phosphorus limitation., *Nature Geoscience*, 13 3, 221-226, 2020.

511 Elrys, A. S., Ali, A., Zhang, H., Cheng, Y., Zhang, J., Cai, Z. C., Mueller, C., and Chang, S. X.: Patterns and drivers of global  
512 gross nitrogen mineralization in soils., *Global Change Biology*, 27, 22, 5950-5962, 2021.

513 Fang, K., Qin, S., Chen, L., Zhang, Q., and Yang, Y.: Al/Fe mineral controls on soil organic carbon stock across Tibetan alpine  
514 grasslands, *Journal of Geophysical Research: Biogeosciences*, 124, 247-259, 2019.

515 Fick, S. E. and Hijmans, R. J.: *Worldclim 2: New 1-km spatial resolution climate surfaces for global land areas.*, 2017.

516 Fierer, N. and Jackson, R. B.: The diversity and biogeography of soil bacterial communities, *Proceedings of the National  
517 Academy of Sciences of the United States of America*, 103, 626-631, 2006.

518 Franco, L. F. M. and Pessôa Filho, P. d. A.: On the solubility of proteins as a function of pH: Mathematical development and  
519 application, *Fluid Phase Equilibria*, 306, 242-250, <https://doi.org/10.1016/j.fluid.2011.04.015>, 2011.

520 Fuka, M. M., Engel, M., Gatteringer, A., Bausenwein, U., Sommer, M., Munch, J. C., and Schloter, M.: Factors influencing  
521 variability of proteolytic genes and activities in arable soils, *Soil biology and Biochemistry*, 40, 1646-1653, 2008.

522 Gislason, S. R., Oelkers, E. H., Eiriksdottir, E. S., Kardjilov, M. I., Gisladottir, G., Sigfusson, B., Snorrason, A., Elefsen, S.,  
523 Hardardottir, J., Torssander, P., and Oskarsson, N.: Direct evidence of the feedback between climate and weathering, *Earth and  
524 Planetary Science Letters*, 277, 213-222, [10.1016/j.epsl.2008.10.018](https://doi.org/10.1016/j.epsl.2008.10.018), 2009.

525 Grayston, S. J., Griffith, G. S., Mawdsley, J. L., Campbell, C. D., and Bardgett, R. D.: Accounting for variability in soil microbial  
526 communities of temperate upland grassland ecosystems, *Soil Biology and Biochemistry*, 33, 533-551,  
527 [https://doi.org/10.1016/S0038-0717\(00\)00194-2](https://doi.org/10.1016/S0038-0717(00)00194-2), 2001.

528 Gu, B., Schmitt, J., Chen, Z., Liang, L., and McCarthy, J. F.: Adsorption and desorption of natural organic matter on iron oxide:  
529 mechanisms and models, *Environmental Science & Technology*, 28, 38-46, 1994.

530 Gu, B., Schmitt, J., Chen, Z., Liang, L., and McCarthy, J. F.: Adsorption and desorption of different organic matter fractions on  
531 iron oxide, *Geochimica et Cosmochimica Acta*, 59, 219-229, [https://doi.org/10.1016/0016-7037\(94\)00282-Q](https://doi.org/10.1016/0016-7037(94)00282-Q), 1995.

532 Hartman, W. H. and Richardson, C. J.: Differential nutrient limitation of soil microbial biomass and metabolic quotients (q CO<sub>2</sub>):  
533 is there a biological stoichiometry of soil microbes?. *PloS one*, 8, e57127, 2013.

534 Hendriksen, N. B., Creamer, R. E., Stone, D., and Winding, A.: Soil exo-enzyme activities across Europe—The influence of  
535 climate, land-use and soil properties, *Applied Soil Ecology*, 97, 44-48, <https://doi.org/10.1016/j.apsoil.2015.08.012>, 2016.

536 Hood-Nowotny, R., Umana, N. H.-N., Inselbacher, E., Oswald- Lachouani, P., and Wanek, W.: Alternative methods for  
537 measuring inorganic, organic, and total dissolved nitrogen in soil, *Soil Science Society of America Journal*, 74, 1018,  
538 [10.2136/sssaj2009.0389](https://doi.org/10.2136/sssaj2009.0389), 2010.

539 Hu, L. T. and Bentler, P. M.: Cutoff Criteria for Fit Indexes in Covariance Structure Analysis: Conventional Criteria Versus New  
540 Alternatives, *Structural Equation Modeling—a Multidisciplinary Journal*, 6, 1-55, [10.1080/10705519909540118](https://doi.org/10.1080/10705519909540118), 1999.

541 Hu, Y., Zheng, Q., Zhang, S., Noll, L., and Wanek, W.: Significant release and microbial utilization of amino sugars and d-amino  
542 acid enantiomers from microbial cell wall decomposition in soils, *Soil Biology and Biochemistry*, 123, 115-125, 2018.

543 Jangid, K., Williams, M. A., Franzluebbers, A. J., Sanderlin, J. S., Reeves, J. H., Jenkins, M. B., Endale, D. M., Coleman, D. C.,  
544 and Whitman, W. B.: Relative impacts of land-use, management intensity and fertilization upon soil microbial community  
545 structure in agricultural systems, *Soil Biology and Biochemistry*, 40, 2843-2853, 2008.

546 Jones, D. L., Owen, A. G., and Farrar, J. F.: Simple method to enable the high resolution determination of total free amino acids  
547 in soil solutions and soil extracts, *Soil Biology and Biochemistry*, 34, 1893-1902, 2002.

548 Kaiser, C., Koranda, M., Kitzler, B., Fuchslueger, L., Schneckner, J., Schweiger, P., Rasche, F., Zechmeister - Boltenstern, S.,  
549 Sessitsch, A., and Richter, A.: Belowground carbon allocation by trees drives seasonal patterns of extracellular enzyme activities  
550 by altering microbial community composition in a beech forest soil, *New Phytologist*, 187, 843-858, 2010.

551 Kaiser, K. and Guggenberger, G.: The role of DOM sorption to mineral surfaces in the preservation of organic matter in soils,  
552 *Organic Geochemistry*, 31, 711-725, [http://dx.doi.org/10.1016/S0146-6380\(00\)00046-2](https://doi.org/10.1016/S0146-6380(00)00046-2), 2000.

553 Kaiser, K. and Guggenberger, G.: Mineral surfaces and soil organic matter, *European Journal of Soil Science*, 54, 219-236,  
554 [10.1046/j.1365-2389.2003.00544.x](https://doi.org/10.1046/j.1365-2389.2003.00544.x), 2003.

555 Kang, H. Z., Xin, Z. J., Berg, B., Burgess, P. J., Liu, Q. L., Liu, Z. C., Li, Z. H., and Liu, C. J.: Global pattern of leaf litter  
556 nitrogen and phosphorus in woody plants, *Annals of Forest Science*, 67, 8, [10.1051/forest/2010047](https://doi.org/10.1051/forest/2010047), 2010.

557 Khare, N., Eggleston, C. M., Lovelace, D. M., and Boese, S. W.: Structural and redox properties of mitochondrial cytochrome c  
558 co-sorbed with phosphate on hematite ( $\alpha$ -Fe<sub>2</sub>O<sub>3</sub>) surfaces, *Journal of colloid and interface science*, 303, 404-414, 2006.

559 Kim, S.: ppcor: Partial and Semi-Partial (Part) Correlation., <https://CRAN.R-project.org/package=ppcor>, 2015.

560 Kirkham, D. and Bartholomew, W.: Equations for following nutrient transformations in soil, utilizing tracer data, *Soil Science  
561 Society of America Journal*, 18, 33-34, 1954.

562 Kleber, M., Mikutta, R., Torn, M., and Jahn, R.: Poorly crystalline mineral phases protect organic matter in acid subsoil horizons,  
563 *European Journal of Soil Science*, 56, 717-725, 2005.

564 Kögel - Knabner, I., Guggenberger, G., Kleber, M., Kandeler, E., Kalbitz, K., Scheu, S., Eusterhues, K., and Leinweber, P.:  
565 Organo - mineral associations in temperate soils: Integrating biology, mineralogy, and organic matter chemistry, *Journal of Plant  
566 Nutrition and Soil Science*, 171, 61-82, [10.1002/jpln.200700048](https://doi.org/10.1002/jpln.200700048), 2008.

567 Koutsoukos, P. G., Norde, W., and Lyklema, J.: Protein adsorption on hematite ( $\alpha$ -Fe<sub>2</sub>O<sub>3</sub>) surfaces, *Journal of Colloid and  
568 Interface Science*, 95, 385-397, [https://doi.org/10.1016/0021-9797\(83\)90198-4](https://doi.org/10.1016/0021-9797(83)90198-4), 1983.

569 Kuo, S.: Phosphorus. p. 869–919. DL Sparks (ed.) *Methods of soil analysis. Part 3. SSSA Book Ser. 5. SSSA, Madison, WI,*  
570 *Phosphorus. p. 869–919. In DL Sparks (ed.) Methods of soil analysis. Part 3. SSSA Book Ser. 5. SSSA, Madison, WI., -, 1996.*

571 La Pierre, K. J., Blumenthal, D. M., Brown, C. S., Klein, J. A., and Smith, M. D.: Drivers of Variation in Aboveground Net  
572 Primary Productivity and Plant Community Composition Differ Across a Broad Precipitation Gradient, *Ecosystems*, 19, 521-533,  
573 [10.1007/s10021-015-9949-7](https://doi.org/10.1007/s10021-015-9949-7), 2016.

574 Lachouani, P., Frank, A. H., and Wanek, W.: A suite of sensitive chemical methods to determine the delta<sup>15</sup>N of ammonium,  
575 nitrate and total dissolved N in soil extracts, *Rapid Commun Mass Spectrom*, 24, 3615-3623, 10.1002/rcm.4798, 2010.

576 Lajtha, K., Driscoll, C., Jarrell, W., and Elliott, E.: Soil phosphorus: characterization and total element analysis, *Standard soil*  
577 *methods for long-term ecological research*. Oxford University Press, New York, 115-142, 1999.

578 Lauber, C. L., Hamady, M., Knight, R., and Fierer, N.: Soil pH as a predictor of soil bacterial community structure at the  
579 continental scale: a pyrosequencing-based assessment, *Applied and Environmental Microbiology*, 2009.

580 Lauber, C. L., Strickland, M. S., Bradford, M. A., and Fierer, N.: The influence of soil properties on the structure of bacterial and  
581 fungal communities across land-use types, *Soil Biology and Biochemistry*, 40, 2407-2415,  
582 <https://doi.org/10.1016/j.soilbio.2008.05.021>, 2008.

583 Leinemann, T., Preusser, S., Mikutta, R., Kalbitz, K., Cerli, C., Höschen, C., Mueller, C. W., Kandeler, E., and Guggenberger, G.:  
584 Multiple exchange processes on mineral surfaces control the transport of dissolved organic matter through soil profiles, *Soil*  
585 *Biology and Biochemistry*, 118, 79-90, <https://doi.org/10.1016/j.soilbio.2017.12.006>, 2018.

586 Loeppert, R. H.: Iron Methods of Soil Analysis. Part 3, in: *Methods of Soil Analysis Part 3*, edited by: Sparks, D. L., SSSA Book  
587 Series, Soil Science Society of America, Inc. & American society of Agronomy, Inc., Madison, WI, 639-664, 1996.

588 Luo, Z., Feng, W., Luo, Y., Baldock, J., and Wang, E.: Soil organic carbon dynamics jointly controlled by climate, carbon inputs,  
589 soil properties and soil carbon fractions - Luo - 2017 - *Global Change Biology* - Wiley Online Library, *Global Change Biology*,  
590 23, 4430 – 4439, 10.1111/gcb.13767, 201.

591 Lützw, M. v., Kögel - Knabner, I., Ekschmitt, K., Matzner, E., Guggenberger, G., Marschner, B., and Flessa, H.: Stabilization of  
592 organic matter in temperate soils: mechanisms and their relevance under different soil conditions—a review, *European Journal of*  
593 *Soil Science*, 57, 426-445, 2006.

594 Martens, D. A. and Loeffelmann, K. L.: Soil amino acid composition quantified by acid hydrolysis and anion chromatography-  
595 pulsed amperometry, *Journal of Agricultural and Food Chemistry*, 51, 6521-6529, 2003.

596 Marty, C., Houle, D., Gagnon, C., and Courchesne, F.: The relationships of soil total nitrogen concentrations, pools and C:N ratios  
597 with climate, vegetation types and nitrate deposition in temperate and boreal forests of eastern Canada, *Catena*, 152, 163-172,  
598 10.1016/j.catena.2017.01.014, 2017.

599 Mikutta, R., Kaiser, K., Dörr, N., Vollmer, A., Chadwick, O. A., Chorover, J., Kramer, M. G., and Guggenberger, G.:  
600 Mineralogical impact on organic nitrogen across a long-term soil chronosequence (0.3–4100 kyr), *Geochimica et Cosmochimica*  
601 *Acta*, 74, 2142-2164, 2010.

602 Mooshammer, M., Wanek, W., Schneckner, J., Wild, B., Leitner, S., Hofhansl, F., Blöchl, A., Hämmerle, I., Frank, A. H., and  
603 Fuchslueger, L.: Stoichiometric controls of nitrogen and phosphorus cycling in decomposing beech leaf litter, *Ecology*, 93, 770-  
604 782, 2012.

605 Moni, C., Chabbi, A., Nunan, N., Rumpel, C., and Chenu, C.: Do iron and aluminium oxides stabilise organic matter in soil? A  
606 multi-scale statistical analysis, from field to horizon. in: *AGU Fall Meeting Abstracts*, 2007, B11G-04.

607 Nierop, K. G., Jansen, B., and Verstraten, J. M.: Dissolved organic matter, aluminium and iron interactions: precipitation induced  
608 by metal/carbon ratio, pH and competition, *Science of the Total Environment*, 300, 201-211, 2002.

609 Noll, L., Zhang, S., and Wanek, W.: Novel high-throughput approach to determine key processes of soil organic nitrogen cycling:  
610 Gross protein depolymerization and microbial amino acid uptake, *Soil Biology and Biochemistry*, 130, 73-81,  
611 <https://doi.org/10.1016/j.soilbio.2018.12.005>, 2019a.

612 Noll, L., Zhang, S., Zheng, Q., Hu, Y., and Wanek, W.: Wide-spread limitation of soil organic nitrogen transformations by  
613 substrate availability and not by extracellular enzyme content, *Soil Biology and Biochemistry*, 133, 37-49,  
614 <https://doi.org/10.1016/j.soilbio.2019.02.016>, 2019b.

615 Norton, K. P., Molnar, P., and Schlunegger, F.: The role of climate-driven chemical weathering on soil production.,  
616 *Geomorphology*, 204, 510-517, 2014.

617 Padbushan, R., Kumar, U., Sharma, S., Rana, D. S., Kumar, R., Kohli, A., Kumari, P., Parmar, B., Kaviraj, M., Sinha, A. K.,  
618 Annapura, K. and Gupta, V. V.: Impact of Land-Use Changes on Soil Properties and Carbon Pools in India: A Meta-analysis,  
619 *Frontiers in Environmental Science*, 722., 2022.

620 Peng, X. and Wang, W.: Stoichiometry of soil extracellular enzyme activity along a climatic transect in temperate grasslands of  
621 northern China, *Soil Biology and Biochemistry*, 98, 74-84, <https://doi.org/10.1016/j.soilbio.2016.04.008>, 2016.

622 Peter J Hernes, R. B., Gregory L Cowie, Miguel A Goñi, Brian A Bergamaschi, John I Hedges.: Tannin diagenesis in mangrove  
623 leaves from a tropical estuary: a novel molecular approach, *Geochimica et Cosmochimica Acta*, 65, 3109-3122, 2001.

624 Prommer, J., Wanek, W., Hofhansl, F., Trojan, D., Offre, P., Urich, T., Schleper, C., Sassmann, S., Kitzler, B., Soja, G., and  
625 Hood-Nowotny, R. C.: Biochar decelerates soil organic nitrogen cycling but stimulates soil nitrification in a temperate arable field  
626 trial, *PLoS One*, 9, e86388, 10.1371/journal.pone.0086388, 2014.

627 Pronk, G. J., Heister, K., and Kögel-Knabner, I.: Is turnover and development of organic matter controlled by mineral  
628 composition?, *Soil Biology and Biochemistry*, 67, 235-244, 2013.

629 Quiquampoix, H.: Mechanisms of protein adsorption on surfaces and consequences for extracellular enzyme activity in soil, in:  
630 *Soil biochemistry*, 171-206, 2000.

631 Quiquampoix, H. and Ratliffe, R. G.: A <sup>31</sup>P NMR study of the adsorption of bovine serum albumin on montmorillonite using  
632 phosphate and the paramagnetic cation Mn<sup>2+</sup>: modification of conformation with pH, *Journal of Colloid and Interface Science*,  
633 148, 343-352, [https://doi.org/10.1016/0021-9797\(92\)90173-J](https://doi.org/10.1016/0021-9797(92)90173-J), 1992.

634 R Development Core Team: R: A language and environment for statistical computing, R Foundation for Statistical Computing  
635 [code], 2008.

636 Reich, P. B. and Oleksyn, J.: Global patterns of plant leaf N and P in relation to temperature and latitude, *Proceedings of the*  
637 *National Academy of Sciences of the United States of America*, 101, 11001-11006, 10.1073/pnas.0403588101, 2004.

638 Rosseel, Y.: *The lavaan tutorial*, 2018.

639 Rousk, J., Bååth, E., Brookes, P. C., Lauber, C. L., Lozupone, C., Caporaso, J. G., Knight, R., and Fierer, N.: Soil bacterial and  
640 fungal communities across a pH gradient in an arable soil, *The ISME journal*, 4, 1340, 2010.

641 Scheel, T., Pritsch, K., Schloter, M., and Kalbitz, K.: Precipitation of enzymes and organic matter by aluminum-Impacts on  
642 carbon mineralization, *Journal of Plant Nutrition and Soil Science*, 171, 900-907, 10.1002/jpln.200700146, 2008.

643 Schulten, H.-R. and Schnitzer, M.: The chemistry of soil organic nitrogen: a review, *Biology and Fertility of Soils*, 26, 1-15, 1997.

644 Sinsabaugh, R. L., Lauber, C. L., Weintraub, M. N., Ahmed, B., Allison, S. D., Crenshaw, C., Contosta, A. R., Cusack, D., Frey,  
645 S., Gallo, M. E., Gartner, T. B., Hobbie, S. E., Holland, K., Keeler, B. L., Powers, J. S., Stursova, M., Takacs - Vesbac, C.,  
646 Waldrop, M. P., Wallenstein, M. D., Zak, D. R., and Zeglin, L. H.: Stoichiometry of soil enzyme activity at global scale, *Ecology*  
647 *Letters*, 11, 1252-1264, 10.1111/j.1461-0248.2008.01245.x, 2008.

648 Six, J. and Jastrow, J. D.: Organic matter turnover, *Encyclopedia of soil science*, 936-942, 2002.

649 Staunton, S. and Quiquampoix, H.: Adsorption and conformation of bovine serum albumin on montmorillonite: Modification of  
650 the balance between hydrophobic and electrostatic interactions by protein methylation and pH variation, *Journal of Colloid and*  
651 *Interface Science*, 166, 89-94, <https://doi.org/10.1006/jcis.1994.1274>, 1994.

652 Wanek, W., Mooshammer, M., Blöchl, A., Hanreich, A., and Richter, A.: Determination of gross rates of amino acid production  
653 and immobilization in decomposing leaf litter by a novel <sup>15</sup>N isotope pool dilution technique, *Soil Biology and Biochemistry*, 42,  
654 1293-1302, 10.1016/j.soilbio.2010.04.001, 2010.

655 Wattel-Koekkoek, E. J. W., van Genuchten, P. P. L., Buurman, P., and van Lagen, B.: Amount and composition of clay-  
656 associated soil organic matter in a range of kaolinitic and smectitic soils, *Geoderma*, 99, 27-49, [https://doi.org/10.1016/S0016-](https://doi.org/10.1016/S0016-7061(00)00062-8)  
657 [7061\(00\)00062-8](https://doi.org/10.1016/S0016-7061(00)00062-8), 2001.

658 Wild, B., Schnecker, J., Barta, J., Capek, P., Guggenberger, G., Hofhansl, F., Kaiser, C., Lashchinsky, N., Mikutta, R.,  
659 Mooshammer, M., Santruckova, H., Shibistova, O., Urich, T., Zimov, S. A., and Richter, A.: Nitrogen dynamics in Turbic  
660 Cryosols from Siberia and Greenland, *Soil Biol Biochem*, 67, 85-93, 10.1016/j.soilbio.2013.08.004, 2013.

661 Xiao, W., Chen, X., Jing, X., & Zhu, B.: A meta-analysis of soil extracellular enzyme activities in response to global change, *Soil*  
662 *Biology and Biochemistry*, 123, 21-32, 2018..

663 Xu, X., Thornton, P. E., & Post, W. M.: A global analysis of soil microbial biomass carbon, nitrogen and phosphorus in terrestrial  
664 ecosystems. *Global Ecology and Biogeography*, 22, 737-749, 2013.

665 Yaalon, D. H.: Soils in the Mediterranean region: what makes them different?, *CATENA*, 28, 157-169,  
666 [https://doi.org/10.1016/S0341-8162\(96\)00035-5](https://doi.org/10.1016/S0341-8162(96)00035-5), 1997.

667 Yang, Y., Fang, J., Ma, W., and Wang, W.: Relationship between variability in aboveground net primary production and  
668 precipitation in global grasslands, *Geophysical Research Letters*, 35, 2008.

669 Zhang, L. and Altabet, M. A.: Amino-group-specific natural abundance nitrogen isotope ratio analysis in amino acids, *Rapid*  
670 *Commun Mass Spectrom*, 22, 559-566, 10.1002/rcm.3393, 2008.

671

672